Effects of Motion Cues on the Training of Multi-Axis Manual Control Skills

Peter M.T. Zaal*
San Jose State University
NASA Ames Research Center
Moffett Field, CA

Xander R.I. Mobertz†
San Jose State University
NASA Ames Research Center
Moffett Field, CA
and
Delft University of Technology
Delft, Netherlands

The study described in this paper investigated the effects of two different hexapod motion configurations on the training and transfer of training of a simultaneous roll and pitch control task. Pilots were divided between two groups which trained either under a baseline hexapod motion condition, with motion typically provided by current training simulators, or an optimized hexapod motion condition, with increased fidelity of the motion cues most relevant for the task. All pilots transferred to the same full-motion condition, representing motion experienced in flight. A cybernetic approach was used that gave insights into the development of pilots' use of visual and motion cues over the course of training and after transfer. Based on the current results, neither of the hexapod motion conditions can unambiguously be chosen as providing the best motion for training and transfer of training of the used multi-axis control task. However, the optimized hexapod motion condition did allow pilots to generate less visual lead, control with higher gains, and have better disturbance-rejection performance at the end of the training session compared to the baseline hexapod motion condition. Significant adaptations in control behavior still occurred in the transfer phase under the full-motion condition for both groups. Pilots behaved less linearly compared to previous single-axis control-task experiments; however, this did not result in smaller motion or learning effects. Motion and learning effects were more pronounced in pitch compared to roll. Finally, valuable lessons were learned that allow us to improve the adopted approach for future transfer-of-training studies.

Nomenclature

A	sinusoid amplitude, deg	n	pilot remnant, deg
e	error signal, deg	n	sinusoid frequency integer factor
F	learning rate	p_0	learning curve initial value
f	forcing function, deg	p_∞	learning curve asymptotic value
H_c	controlled dynamics	r^2	coefficient of determination
H_f	motion washout response	s	Laplace operator
H_{ol}	open-loop response	t	time, s
H_p	pilot response	T_L	pilot lead time constant, s
i_r	run number	T_m	measurement time, s
K_{trs}	c.g. translational acceleration gain, $-$	u	pilot control input, deg
K_{rtl}	c.g. to p.s. translational acceleration gain, $-$	y_r	learning curve value
K_m	pilot motion gain, $-$	δ_a	aileron deflection, deg
K_f	motion washout gain, $-$	δ_e	elevator deflection, deg
K_v	pilot visual gain, $-$	ζ_f	motion washout damping ratio, $-$
K_s	stick gain, $-$	ζ_{nm}	neuromuscular damping, $-$
k	sinusoid index	θ	pitch angle, deg
N	number of sinusoids	τ	pilot processing delay, s

*Senior Research Engineer, Human Systems Integration Division, NASA Ames Research Center, P.O. Box 1, Moffett Field, CA, 94035 / Mail Stop 262-2; peter.m.t.zaal@nasa.gov. Member.

†Research Scholar, Human Systems Integration Division, NASA Ames Research Center, P.O. Box 1, Moffett Field, CA, 94035, and Delft University of Technology, Delft, Netherlands; xander@mobertz.com.

ϕ	roll angle, deg
ϕ	sinusoid phase, rad
φ_m	phase margin, deg
ω	frequency, rad s^{-1}
ω_c	crossover frequency, rad s^{-1}
ω	sinusoid frequency, rad s^{-1}
ω_m	measurement time base frequency, rad s^{-1}
ω_f	motion washout break frequency, rad s^{-1}
ω_{nm}	neuromuscular frequency, rad s^{-1}

Subscripts

d	disturbance
e	error
m	motion
t	target
v	visual
θ	pitch
ϕ	roll

Abbreviations

c.g.	aircraft center of gravity
MLE	Maximum Likelihood Estimation
PFD	primary flight display
p.s.	pilot station
RMS	root mean square
VAF	variance accounted for
VMS	Vertical Motion Simulator

I. Introduction

The study described in this paper investigates the effects of two different motion conditions on the training and transfer of training of multi-axis (roll and pitch) manual control behavior. The utility of simulator motion for the training of pilot manual control skills in flight simulators is still very much debated.[1] In addition, very limited motion cueing guidelines and criteria are available to objectively tune simulator motion for pilot training.[2,3] The effects of motion system hardware and cueing characteristics on human manual control behavior and performance are relatively well understood.[2,4–6] However, there is currently limited understanding of how these effects influence the *acquisition* of manual control skills in motion-base simulators and the transfer of the learned skills to the operational environment in an aircraft. A better understanding of how motion affects the training and transfer of training of manual control skills is required to develop guidelines and criteria for simulator motion cueing optimized for the training of manual control skills and better transfer of training.

The identification and modeling of human manual control behavior using a cybernetic approach has been used in many previous research efforts investigating the effects of motion on manual control behavior and performance.[4,5,7,8] The advantage of this approach is that it enables analyzing how human controllers integrate visual and motion cues to make a control action. The same approach can give more insights into how manual control behavior and the use of both visual and motion cues develop during training and transfer after training. Only few studies have used this approach in the context of training and the ones that did used single-axis control tasks,[9,10] or looked at the effects of elementary variations of visual and motion cues, such as the effects of training with and without motion.[11,12] Even though these studies are crucial for our understanding of the acquisition of manual control skills, their results might not directly apply to the training and transfer of training of manual control skills for aircraft flying tasks that mostly require control and result in motion cues in multiple axes simultaneously.

This paper adds to the literature as follows: 1) a cybernetic approach was used to investigate the training and transfer of training of manual control skills in a *multi-axis* control task with aircraft dynamics, a task more comparable to manually flying an aircraft, 2) this study was part of a larger research effort to develop motion cueing guidelines for stall recovery training, and, therefore, aircraft dynamics of an aircraft close to the stall point were used, and 3) a quasi-transfer-of-training experiment was conducted in the Vertical Motion Simulator (VMS), the world's largest vertical displacement simulator, in which general aviation pilots trained for the task under one out of two hexapod motion conditions and then transferred to a full motion condition, closer to motion in flight, which utilized the entire VMS motion envelope.

The paper provides details on the roll-pitch control task, aircraft dynamics, and pilot model in Section II. Next, the experimental setup will be discussed in Section III. Results will be given in Section IV and will be discussed in Section V, after which the paper ends with the main conclusions in Section VI.

II. Control Task

The effects of motion cues on the training and transfer of training of multi-axis manual control skills were assessed in a simultaneous roll and pitch target-following disturbance-rejection task. Fig. 1 depicts a diagram of the closed-loop control task.

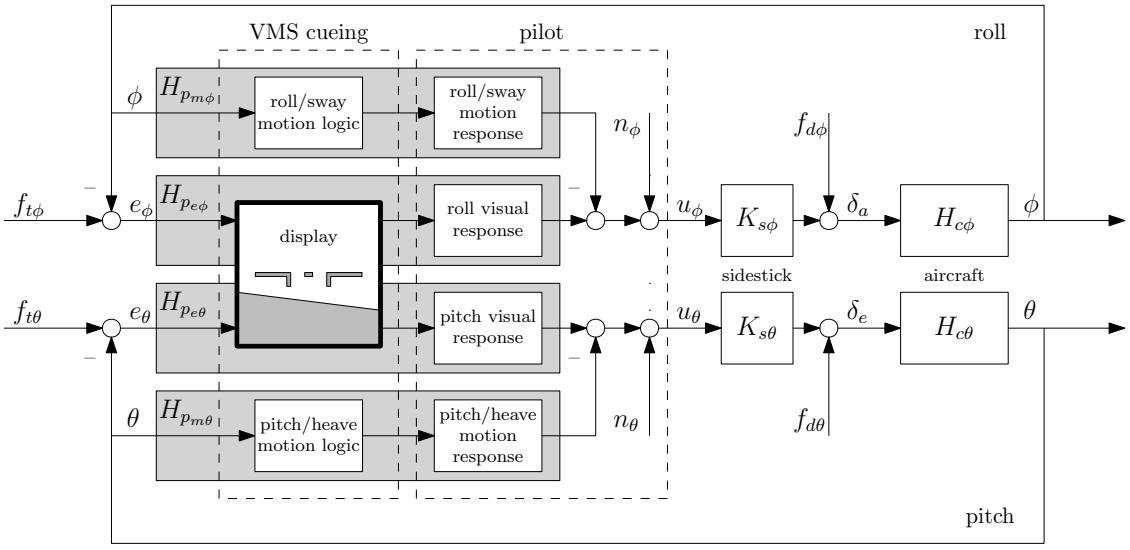

Figure 1. Multi-axis closed loop control task.

Pilots' task was to simultaneously minimize roll and pitch errors, e_ϕ and e_θ, on a compensatory display similar to a primary flight display (PFD). The roll and pitch errors were the differences between roll and pitch target forcing functions, $f_{t\phi}$ and $f_{t\theta}$, and roll and pitch attitudes, ϕ and θ, respectively. The roll and pitch attitudes were the outputs of the roll and pitch dynamics, $H_{c\phi}$ and $H_{c\theta}$, combined, constituting the controlled aircraft dynamics. No cross coupling was present between the roll and pitch dynamics; that is, roll inputs did not result in pitch attitude changes and vice versa. Pilots controlled the aircraft dynamics using a sidestick with roll gain $K_{s\phi}$ and pitch gain $K_{s\theta}$. Disturbance forcing functions $f_{d\phi}$ and $f_{d\theta}$ were added to the stick outputs, exciting the aircraft dynamics similarly to atmospheric turbulence. In addition to visual cues, pilots were also provided with roll and sway motion cues, and pitch and heave motion cues, resulting from changes in roll and pitch attitudes, respectively.

The two forcing functions in the closed control loop in each axis allowed for the identification of pilots' visual and motion responses, H_{p_e} and H_{p_m}, in both axes (Fig. 1). The control inputs of the pilot, u_ϕ and u_θ, are a combination of the outputs of these linear response functions and remnant signals, n_ϕ and n_θ, that account for nonlinear behavior and noise. Note that the identified pilot motion response functions, in reality, also include simulator motion logic and motion system dynamics. The same holds for the visual response functions, which include display dynamics. In addition, the pilot motion response functions are a combination of responses resulting from different perceptual modalities, such as vestibular, somatosensory, and proprioceptive.

The remainder of this section discusses each aspect of the control task in more detail.

II.A. Controlled Aircraft Dynamics

The controlled aircraft dynamics were of a medium-sized transport aircraft, similar in size to a Boeing 757. The gross weight of the airplane was set to 185,800 lbs. The aircraft dynamics were linearized at a flight condition close to the stall point, at an altitude of 41,000 ft and an airspeed of 150 kts. The linearized roll and pitch dynamics were defined by Equations 1 and 2, respectively.

$$H_{c\phi}(s) = \frac{\phi}{\delta_a} = \frac{0.76773\,(s^2 + 0.2195\,s + 0.5931)}{(s + 0.7363)\,(s - 0.01984)\,(s^2 + 0.1455\,s + 0.6602)} \tag{1}$$

$$H_{c\theta}(s) = \frac{\theta}{\delta_e} = \frac{0.33282\,(s^2 + 0.09244\,s + 0.002886)}{(s^2 - 0.01388\,s + 0.004072)\,(s^2 + 0.446\,s + 0.4751)} \tag{2}$$

II.B. Pilot Model

According to the crossover model theorem, a human operator adjusts his or her control behavior to the controlled dynamics such that the combined human-operator controlled-dynamics open-loop response approximates a single

integrator near the crossover frequency.[13] The characteristics of the controlled dynamics in Equations 1 and 2 require a human operator to generate lead at higher frequencies. Taking this into account, the human operator visual and motion response functions are given by Equations 3 and 4, respectively. Note that any nonlinearities in behavior are captured in the remnant signal n (Fig. 1).

$$H_{p_e}(s) = K_v(1 + T_L s)e^{-\tau_v s}\frac{\omega_{nm}^2}{s^2 + 2\zeta_{nm}\omega_{nm}s + \omega_{nm}^2} \tag{3}$$

$$H_{p_m}(s) = sK_m e^{-\tau_m s}\frac{\omega_{nm}^2}{s^2 + 2\zeta_{nm}\omega_{nm}s + \omega_{nm}^2} \tag{4}$$

In Equations 3 and 4, equalization dynamics are characterized by the visual gain K_v, motion gain K_m, and the visual lead time constant T_L. Human controller limitations are captured by the visual delay τ_v, motion delay τ_m, neuromuscular frequency ω_{nm}, and neuromuscular damping ζ_{nm}. Estimating these parameters over the course of training and after transfer allows for quantification and characterization of the acquisition and transfer of pilot multi-axis manual control skills.

In the frequency domain, pilot performance in attenuating the target and disturbance forcing functions can be determined by the phase margins and crossover frequencies of the target and disturbance open-loop dynamics, respectively.[14] Using the control diagram in Fig. 1, the target and disturbance open-loop responses are given by:

$$H_{ol_t}(s) = \frac{H_{p_e}(s)\,K_s H_c(s)}{1 + H_{p_m}(s)\,K_s H_c(s)} \tag{5}$$

$$H_{ol_d}(s) = \left[H_{p_e}(s) + H_{p_m}(s)\right] K_s H_c(s) \tag{6}$$

The disturbance and target crossover frequencies (ω_{c_d} and ω_{c_t}) are frequencies where the magnitude of the disturbance and target open-loop responses is 1.0. At these crossover frequencies, phase differences from -180 degrees are the phase margins (φ_{m_d} and φ_{m_t}).

II.C. Simulator Motion

The experiment used the standard VMS motion algorithm and hardware for all motion configurations. The equivalent time delays of the VMS motion system for the pitch, roll, yaw, longitudinal, lateral and vertical axes are 47, 68, 48, 50, 69 and 67 ms, respectively. More details about the motion algorithm are provided in Ref. 15. The VMS motion logic consists of second-order high-pass washout filters to attenuate the rotational and translational aircraft model accelerations:

$$H_f(s) = K_f\frac{s^2}{s^2 + 2\zeta_f\omega_f s + \omega_f^2} \tag{7}$$

where K_f is the motion washout gain, and ζ_f and ω_f are the washout damping ratio and break frequency, respectively.

The acquisition of manual control skills in the multi-axis control task in Fig. 1 was analyzed in a transfer-of-training experiment with two training-motion conditions. The two training-motion conditions, baseline hexapod motion (HB) and optimized hexapod motion (HO), had motion logic parameters tuned such that the simulated motion would fit in the motion envelope of a typical hexapod motion-base simulator with 60-inch legs. For this purpose, an actuator extension algorithm was implemented in the VMS that calculated the hexapod actuator extensions resulting from the aircraft motions, allowing for the tuning and monitoring of the motion in a much smaller hexapod motion space.[16] After training, every pilot was transferred to a true aircraft motion condition (FM). The motion logic parameters in this condition were tuned such that the full VMS motion envelope was utilized.

The different motion conditions not only differed in motion logic parameter settings, but also in the type of translational accelerations simulated. Translational accelerations at the pilot station are a combination of translational accelerations of the aircraft's center of gravity (c.g.) and translational accelerations as a result of the pilot station (p.s.) rotating with respect to the center of gravity (Fig. 2). Gains on each of the translational acceleration components (K_{trs} and K_{rtl}) allowed for a different weighting of each component.

The baseline hexapod motion condition HB simulated motion provided by a typical hexapod motion simulator. The motion response of the VMS motion system for this condition was matched to the average response of a statistical sample of eight simulators using the Objective Motion Cueing Test (OMCT).[17] Both the translational acceleration components from the c.g. and as a result of rotations with respect to the c.g. were simulated in this condition. The

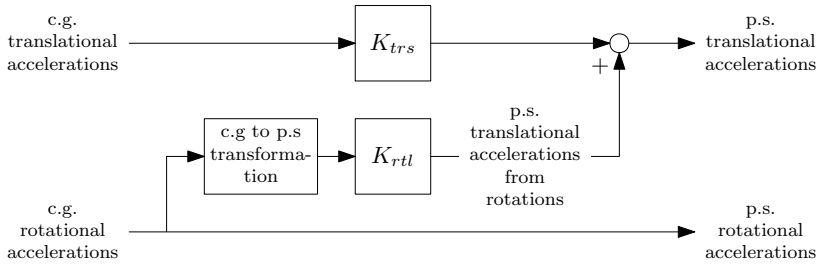

Figure 2. Transformation from center of gravity to pilot station accelerations.

Table 1. Motion logic parameters.

Motion Component Gains			
	HB	HO	FM
K_{trs}	1.00	0.00	1.00
K_{rtl}	1.00	1.00	1.00

Washout Gains			
	HB	HO	FM
K_{fx}	0.58	0.60	0.60
K_{fy}	0.72	1.00	1.00
K_{fz}	0.63	1.00	1.00
K_{fp}	0.74	1.00	1.00
K_{fq}	0.86	1.00	1.00
K_{fr}	0.63	1.00	1.00

Washout Break Frequencies			
	HB	HO	FM
ω_{fx}	2.04	0.50	0.50
ω_{fy}	0.87	0.35	0.35
ω_{fz}	2.76	0.20	0.20
ω_{fp}	1.06	0.20	0.20
ω_{fq}	0.49	0.20	0.20
ω_{fr}	0.77	0.20	0.20

Washout Damping Ratios			
	HB	HO	FM
ζ_{fx}	0.58	0.71	0.71
ζ_{fy}	1.57	0.71	0.71
ζ_{fz}	1.10	0.71	0.71
ζ_{fp}	1.18	0.71	0.71
ζ_{fq}	1.22	0.71	0.71
ζ_{fr}	1.10	0.71	0.71

optimized hexapod motion condition HO only simulated the translational accelerations as a result of rotations with respect to the c.g. Taking out the c.g. component of the translational accelerations resulted in a condition where hardly any attenuation of the motion was required, leading to washout gains of 1.00 and break frequencies of 0.20 for most degrees of freedom. The full motion condition FM allowed for the simulation of both translational acceleration components with the motion logic parameter settings of condition HO; that is, with minimal attenuation.

The motion parameters for all motion conditions are provided in Table 1. Details on the tilt coordination were omitted from this discussion for brevity; however, tilt coordination was present in each motion configuration.

II.D. Forcing Functions

The target and disturbance forcing functions were sum-of-sines signals defined by Equation 8, where $A_{d,t}(k)$, $\omega_{d,t}(k)$, and $\phi_{d,t}(k)$ indicated the amplitude, frequency and phase of the k^{th} sine in f_d or f_t respectively. $N_{d,t}$ represents the number of sine waves.

$$f_{d,t}(t) = \sum_{k=1}^{N_{d,t}} A_{d,t}(k) sin[\omega_{d,t}(k)t + \phi_{d,t}(k)] \tag{8}$$

Subscripts d and t are used to distinguish between the disturbance and target forcing function, respectively. The f_d and f_t signals for both pitch and roll consist of ten individual sinusoids each with different amplitudes, frequencies, and phases. A summary of all forcing function properties in roll and pitch can be found in Table 2.

The sinusoid frequencies were all integer multiples of the measurement time base frequency, $\omega_m = 2\pi/T_m = 0.0767$ rad/s. $T_m = 81.92$ s was the measurement time used for the experiment. The selected integer multiples were used in a number of earlier experiments and ensured that the ten sinusoid frequencies in each signal covered the frequency range of human control at regular intervals on a logarithmic scale.

In order to determine the amplitudes of the individual sines for both the target and the disturbance forcing functions, a second-order low-pass filter was used.[4] This second-order filter reduced the magnitude of the amplitudes at higher frequencies, yielding a tracking task that is not too difficult.

The amplitude distributions $A_{t\theta}(k)$ and $A_{d\theta}(k)$ for the pitch axis were scaled to obtain a variance for $f_{t\theta}$ of 0.1 deg^2, and a variance for $f_{d\theta}$ of 0.4 deg^2. For roll, the amplitude distributions $A_{t\phi}(k)$ and $A_{d\phi}(k)$ were scaled such that the variance was 0.4 and 1.6 deg^2 for $f_{t\phi}$ and $f_{d\phi}$, respectively. The variances of the roll forcing functions were four times as high as the variances of the pitch forcing functions, as pitch errors are easier to see than roll errors on a PFD.[18] Note that the ratios of the disturbance-forcing-function to target-forcing-function variances were the same in both axes. This ensured pilots' task was mainly a disturbance-rejection task for both controlled axes.

Table 2. Forcing function properties.

Roll								Pitch							
Disturbance, $f_{d\phi}$				Target, $f_{t\phi}$				Disturbance, $f_{d\theta}$				Target, $f_{t\theta}$			
$n_{d\phi}$ –	$\omega_{d\phi}$ rad s^{-1}	$A_{d\phi}$ deg	$\phi_{d\phi}$ rad	$n_{t\phi}$ –	$\omega_{t\phi}$ rad s^{-1}	$A_{t\phi}$ deg	$\phi_{t\phi}$ rad	$n_{d\theta}$ –	$\omega_{d\theta}$ rad s^{-1}	$A_{d\theta}$ deg	$\phi_{d\theta}$ rad	$n_{t\theta}$ –	$\omega_{t\theta}$ rad s^{-1}	$A_{t\theta}$ deg	$\phi_{t\theta}$ rad
3	0.230	0.006	-1.714	4	0.307	0.866	-2.220	5	0.384	0.013	-1.824	6	0.460	0.506	0.458
7	0.537	0.017	-0.527	9	0.690	0.742	-1.429	11	0.844	0.011	0.906	13	0.997	0.310	-0.205
15	1.151	0.018	0.787	17	1.304	0.447	-1.154	19	1.457	0.024	0.502	21	1.611	0.175	-1.588
23	1.764	0.030	-0.375	25	1.918	0.256	2.296	27	2.071	0.032	-2.291	29	2.224	0.108	1.830
37	2.838	0.040	2.525	41	3.145	0.138	-0.822	44	3.375	0.041	-3.056	45	3.452	0.053	2.619
51	3.912	0.045	2.404	53	4.065	0.092	-0.086	55	4.218	0.046	-1.895	56	4.295	0.037	-0.839
71	5.446	0.053	2.289	73	5.599	0.057	-0.902	75	5.752	0.053	-1.111	76	5.829	0.024	-1.640
101	7.747	0.067	1.363	103	7.900	0.036	2.989	105	8.053	0.067	-0.817	106	8.130	0.015	1.345
137	10.508	0.089	1.635	139	10.661	0.027	0.436	141	10.815	0.089	-2.539	142	10.891	0.011	-2.511
191	14.650	0.134	-1.266	194	14.880	0.021	1.468	192	14.726	0.131	-1.243	195	14.956	0.009	2.191

To determine the forcing function phase distributions, numerous sets of phases were generated. Two sets of phases were chosen for the target and disturbance forcing functions that yielded signals with a Gaussian-like distribution and an average crest factor.[19]

III. Experimental Design

III.A. Method

III.A.1. Experimental Conditions

To observe the effects of training, pilots participated in both a training and transfer session. The motion in the training session was tuned such that it could be replicated on a hexapod simulator (Section II.C). Pilots were divided between two groups and either conducted their training using a baseline hexapod (HB) or optimized hexapod (HO) motion condition. In the transfer session the full motion condition (FM) was always used. The training motion condition was the only independent variable of this experiment. A summary of the motion conditions used is given in Table 3.

Table 3. Experimental conditions.

	Motion Condition	
	Training (day 1)	Transfer (day 2)
Pilot Group HB	HB	FM
Pilot Group HM	HO	FM

III.A.2. Apparatus

The experiment was conducted in the VMS, the world's largest vertical displacement simulator. More details about this simulator can be found in Ref. 15. This experiment used the rotorcraft cab (R-CAB), see Fig. 3.[20] The pilot was positioned in the middle of the cab, and controlled both the pitch and roll degrees of freedom using a joystick positioned on the right side, see Fig. 4. A simplified PFD was positioned in front of the pilot, which displayed the pitch and roll errors (Fig. 5). The out-of-window view was disabled, and covered with blinds to prevent visual distractions. Other lights in the cockpit were also covered.

III.A.3. Participants

Twenty-four general aviation pilots participated in the experiment, of which three pilots had more than 1,500 actual flight hours. The most experienced pilot had 4,100 flight hours. The average number of flight hours was 556 with a standard deviation of $\pm$ 1,078 hours. Furthermore, pilots had an average of 62 hours fixed-base simulator experience, with a standard deviation of $\pm$ 169 hours. Most pilots had flown an average of 75 hours in the past six months, with a standard deviation of 118 hours. The youngest pilot was 19 years old, the oldest 62. On average, the age was 29.3 years, with a standard deviation of $\pm$ 10 years. All participants were comfortable with operating the joystick with their right hand.

Figure 3. Vertical Motion Simulator.

Figure 4. Cockpit setup.

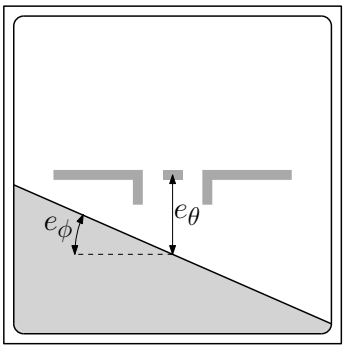

Figure 5. Primary flight display.

III.A.4. Procedures

Prior to the experiment pilots received a thorough briefing, providing an explanation of the task and how controls were to be operated. Pilots were instructed to continuously try to improve their performance, as indicated by a score appearing in the lower right corner of the PFD at the end of each run. The score was the sum of the root mean square (RMS) of the roll and pitch errors. A smaller score indicated a better overall performance throughout that particular run. Pilots were made aware of the best score out of all previous participants to provide motivation. In order to facilitate the identification of pilot control behavior, pilots were instructed to give smooth, continuous inputs. Furthermore, pilots were given specifics of the number of runs and breaks during the experiment. Finally, pilots were asked to fill out a short questionnaire, mainly asking about their experience in terms of simulator and flight hours.

Each pilot conducted the experiment over two consecutive days, either in the morning or in the afternoon. The first day started with a briefing as discussed above, after which a safety briefing of the VMS was given. Next, a training session commenced with one of two training conditions, as described in Section III.A.1. Each pilot was assigned to one of the training conditions randomly. On the second day, participants conducted a transfer session with the full motion condition. After this second session, any questions that the pilots may have had regarding the purpose of the experiment were answered. Both the training and transfer sessions consisted of 60 runs lasting 90 seconds each. Short breaks were given between each run in which pilots remained in the simulator. Three longer brakes of approximately ten minutes were given between intervals of 15 runs.

III.A.5. Dependent Measures

In this study, 24 objective dependent measures were analyzed. These dependent measures were calculated to gain insight into the effects of the training-motion conditions on the development of pilot performance and control behavior during the training and transfer sessions.

The pilot visual and motion transfer functions given by Equations 3 and 4, respectively (Section II.B), contain seven parameters for each axis of control; $K_{v\theta}$, $K_{v\phi}$, $T_{L\theta}$, $T_{L\phi}$, $\tau_{v\theta}$, $\tau_{v\phi}$, $K_{m\theta}$,$K_{m\phi}$, $\tau_{m\theta}$, $\tau_{m\phi}$, $\zeta_{nm\theta}$, $\zeta_{nm\phi}$, $\omega_{nm\theta}$ and $\omega_{nm\phi}$. The control signal variance accounted for (VAF) was calculated for both the roll and pitch axes, VAF_ϕ and VAF_θ, as a measure of the accuracy of the pilot model in describing the measured control signal data.

Furthermore, pilot control performance and intensity were defined in terms of the RMS of the error and control signals, respectively: RMS_{e_θ}, RMS_{e_ϕ}, RMS_{u_θ} and RMS_{u_ϕ}. Finally, the open-loop responses of Equations 5 and 6 were used to calculate the target and disturbance crossover frequencies ω_{c_t} and ω_{c_d}, and phase margins φ_{m_t} and φ_{m_d}, in both the roll and pitch axes.

III.A.6. Data Analysis

Pilots performed 60 runs per session. The RMS values of the error and control signals were calculated for every single measurement run. In order to reliably estimate the seven pilot model parameters in each axis, data from five consecutive runs were averaged in order to minimize the influence of pilot remnant. The averaged data were then used for parameter estimation using Maximum Likelihood Estimation (MLE). First, a genetic algorithm was used to estimate initial parameter values, after which a Gauss-Newton optimization was used to refine the results.[21] This procedure was repeated 25 times for each data point after which the solution with the highest likelihood was chosen.

Parameter values outside of two standard deviations from the mean were considered outliers and were removed from the data set. If possible, outliers were replaced by an alternative MLE solution from the set of 25 with the next highest likelihood. Crossover frequencies and phase margins were calculated for each final MLE parameter solution.

In order to clearly visualize trends in the results found, dependent measures for each pilot group were averaged after which an exponential decay function, representing a learning curve, was fit onto the averaged data. The learning curve is defined by Equation 9, in which p_0 represents the value of the dependent measure at the start of the training or transfer sessions, p_∞ the asymptotic value towards the end of the sessions, and F the learning rate. Finally, i_r represents the run number. The values for these variables were estimated using Matlab's `fmincon` function. The coefficient of determination r^2 was determined to evaluate the goodness of fit. R-squared is always between 0 and 1, with 0 indicating that the learning curve explains none of the variability of the observations, and 1 indicating that the model explains all the variability of the observations.

$$y_r(i_r) = p_\infty + (1 - F)^{i_r}(p_0 - p_\infty) \tag{9}$$

III.B. Hypotheses

For tracking tasks with controlled elements requiring lead equalization, such as those in the current study, motion feedback is typically used by human controllers to reduce the amount of visual lead that needs to be generated.[22] Furthermore, the extent to which such motion feedback is used by human controllers is affected by the quality of the motion cues important to the task. Attenuation of these motion cues, either by scaling or high-pass filtering, results in human manual control with lower gains and increased visual lead generation (higher T_L), which typically results in worse task performance.[4,6,23] Similar effects of motion were also observed in quasi-transfer-of-training experiments using single-axis manual control tasks.[11,12] Based on these previous observations, the following hypotheses were formulated for the current experiment:

H1: Pilots were expected to learn faster under the optimized hexapod motion condition. In addition, pilot control behavior and performance for motion group HO at the start of the transfer session was expected to be more similar to control behavior and performance at the end of training under HO motion. Pilots having trained under motion condition HB were thought to adapt slower to the full-motion condition in the transfer phase. At the end of the transfer phase with full motion, pilot control behavior and performance was expected to be similar for both groups.

H2: After training under the motion condition with optimized hexapod motion (HO), pilots were expected to generate less visual lead, control with higher gains, and, as a result, perform better compared to the baseline hexapod motion condition (HB).[4,23] Pilot equalization parameters and performance at the end of the transfer session with full motion were expected to be similar to the equalization parameters and performance at the end of training with the optimized hexapod motion condition. Differences in pilot limitation parameters between the motion conditions were expected to be minimal.

H3: Pilots were hypothesized to behave more nonlinearly in a multi-axis control task compared to a single-axis control task due to periodic sampling between the two axes.[24] This was expected to result in lower VAF values compared to the single-axis experiments used in previous studies. As a result, the effects of motion in the multi-axis control task were expected to be less pronounced compared to the effects in single-axis control tasks. For the same reason, learning effects were expected to be smaller compared to those observed in transfer-of-training experiments with single-axis tasks.

H4: The effects of motion in the pitch axis were expected to be more pronounced and consistent than in the roll axis.[18] Due to the nature of a PFD, pitch errors are easier to observe than roll errors. With pilots' increased focus on pitch, motion and learning effects were expected to be larger than in roll.

IV. Results

This section provides the experimental results of 19 out of 24 pilots that participated in the experiment. Data from the five pilots excluded from the analysis did not allow for reliable MLE parameter estimates. Of the 19 pilots, nine pilots conducted the training with baseline hexapod motion, whereas ten pilots conducted the training with optimized hexapod motion.

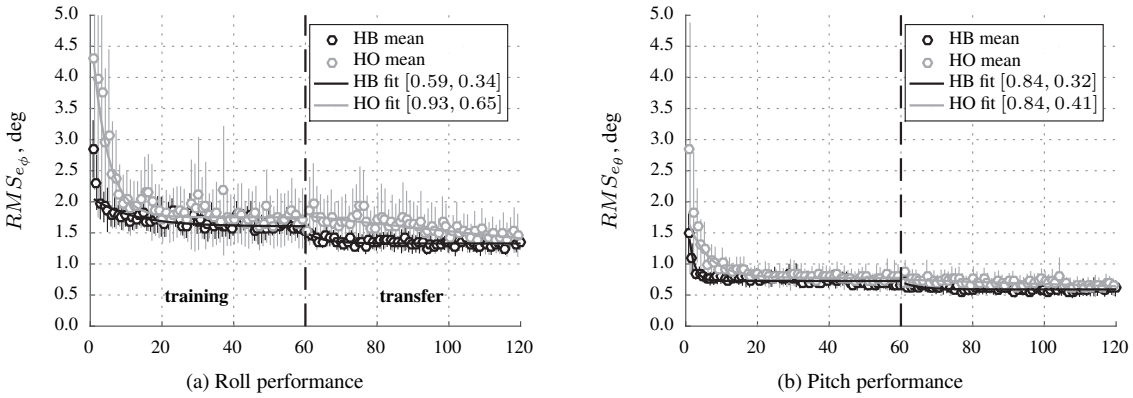

(a) Roll performance (b) Pitch performance

Figure 6. Pitch Roll tracking error variance with disturbance, target and remnant contributions.

Throughout this section, data for the roll axis are presented on the left side of each figure and data for the pitch axis on the right side. Results for the baseline hexapod motion condition HB is presented in black and results for HO are presented in grey. The circle markers in each graph represent the average value over all pilots of a particular group. Error bars in corresponding colors indicate the 95% confidence intervals. The average values were used to fit the learning curve described in Section III.A.6. The learning curves are depicted by black and grey continuous lines for HB and HO, respectively. The coefficient of determination (r^2), a measure of how well observations were replicated by the learning curve, are shown in the legends with the following organization [r^2(training), r^2(transfer)].

IV.A. Tracking Performance and Control Activity

Pilot tracking performance is defined by the RMS of the roll and pitch errors displayed on the PFD. A lower RMS_e indicates better performance. The results for roll and pitch tracking performance are shown in Figures 6a and 6b, respectively. Figures 6a and 6b show that roll and pitch tracking performance steadily improved over the course of the training and transfer sessions, and that performance was similar for both groups. The group of pilots training with HB motion showed a steeper improvement in roll and pitch performance in the training phase and steeper improvement in roll performance in the transfer phase. This means that the group training with HB motion more quickly reached asymptotic performance levels. The group training with HO motion showed a more gradual increase in roll performance in the transfer phase, to such an extent that stable performance was not yet reached at the end the transfer session. Note that in both the training and transfer phases tracking performance in pitch was better than in roll for both pilot groups. This result has also been observed in other multi-axis control studies.[18, 24, 25]

Pilot control activity for roll and pitch are shown in Figures 7a and 7b, respectively. A lower RMS_u indicates lower control activity. Figures 7a and 7b show that control activity decreased over the course of training. This behavior

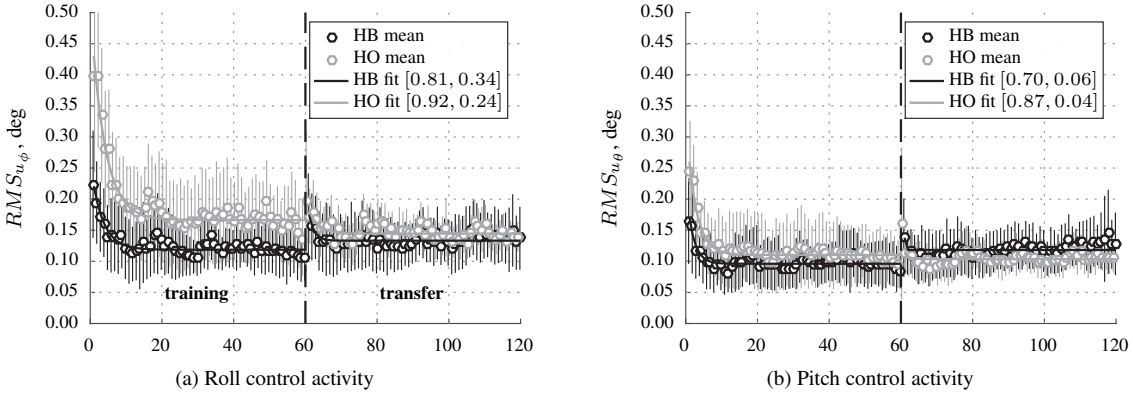

(a) Roll control activity (b) Pitch control activity

Figure 7. Pitch Roll control input variance with disturbance, target and remnant contributions.

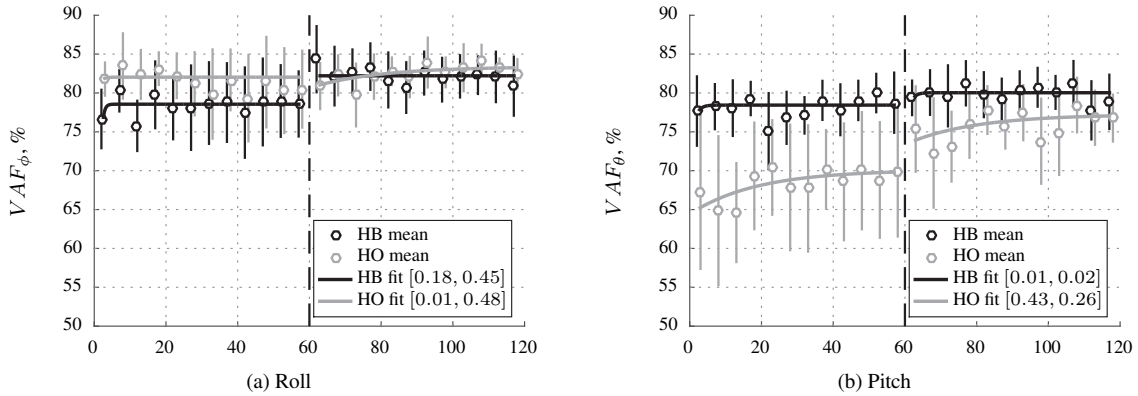

(a) Roll (b) Pitch

Figure 8. Variance Accounted For.

was not expected based on previous training studies, for which control activity increased when training with motion.[12] The RMS of the roll control input during training was higher for HO and control activity at the end of training was more similar to that after transfer. The group training with HB motion showed an increase in roll control intensity after the training phase. In pitch, control activity was similar for both groups and in both phases of the experiment. Pitch control activity increased slightly in the transfer phase for the HB motion group. In the training phase, control activity was higher in the roll axis; however, in the transfer phase, control activity was more similar between the two axes.

IV.B. Variance Accounted For

The linear pilot model as described in Section II.B explains pilot control behavior to a limited extent only. The extent to which the variance of the pilot control signal can be accounted for by this model is indicated by the VAF.

Fig. 8a indicates the VAF of the roll control signal is approximately constant over the course of training and transfer for both groups. The roll VAF for the HO motion group is similar in the transfer and training phases of the experiment. The HB motion group has a slightly lower roll VAF in the training phase, indicating the presence of higher levels of remnant. The results for each group in the pitch axis are opposite to those of the roll axis (Fig. 8b). The pitch VAF for the HB motion group is similar in the transfer and training phases of the experiment, while the pitch VAF of the HO group is lower during the training phase than during the transfer phase. In addition, the pitch VAF is steadily increasing during training and after transfer for the HO motion group. Only towards the end of the transfer phase are the pitch VAFs of both groups similar.

Comparing Figures 8a and 8b reveals that for the HB motion group, the VAF is similar in the roll and the pitch axes. For the HO motion group the VAF is significantly higher in the roll axis. Note that the error bars are significantly larger for the HO motion group in the pitch axis, indicating a larger variability between pilots.

IV.C. Pilot Model Parameters

The evolution of pilot model parameters during the training and transfer sessions can provide more insight in pilots' learning process. The parameters were estimated using the method explained in section III.A.6.

The pilot equalization parameters for the roll and pitch axes are given in Fig. 9. Figures 9a and 9b depict the pilot visual gain for the roll and pitch axes, respectively. In the roll axis, the visual gain of both groups remained stable throughout the training phase. The roll visual gain for the HO motion group is slightly higher than for the HB motion group. At the beginning of the transfer phase, K_v is similar to the training phase for HO in the roll axis; however, K_v increased for HB compared to the training phase. The roll visual gain then increased for both groups over the course of the transfer phase. The roll visual gain did not reach an asymptotic level after 60 evaluation runs. In the pitch axis, K_v increased for both groups during both the training and transfer phases. The visual gains are higher and their error bars are much larger in the pitch axis compared to the roll axis.

The lead time constants for the roll and pitch axes are depicted in Figures 9c and 9d. In both roll and pitch, the visual lead time constant for the HO motion group is lower compared to the HB motion group in the training phase, indicating a decreased use of visual rate information. In addition, T_L decreased for HO over the course of training, while remaining approximately constant for HB. At the beginning of the transfer phase, the visual lead time constant

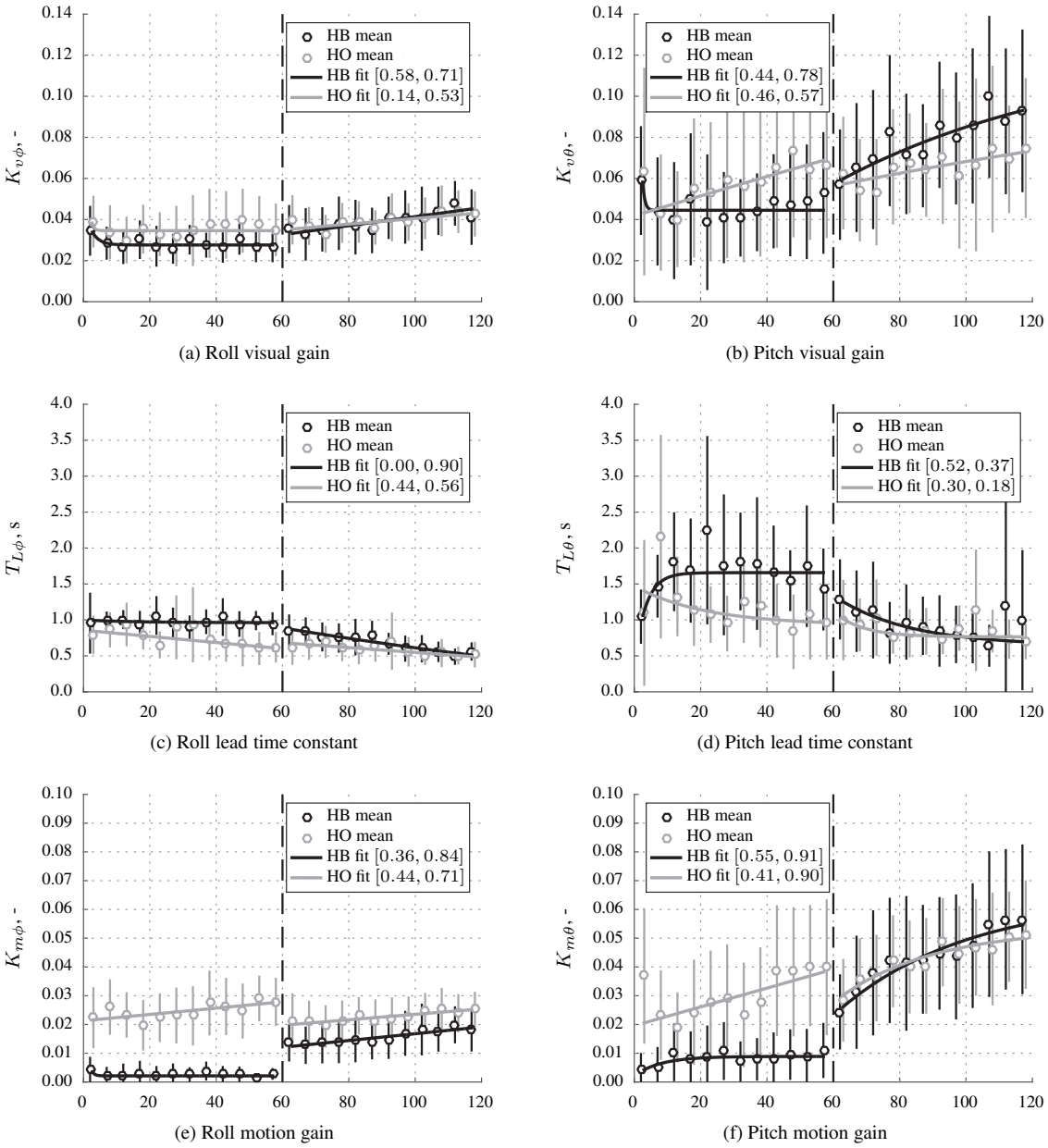

(a) Roll visual gain

(b) Pitch visual gain

(c) Roll lead time constant

(d) Pitch lead time constant

(e) Roll motion gain

(f) Pitch motion gain

Figure 9. Equalization parameters.

for the HO motion group was more similar to that at the end of training. For both motion groups, T_L decreased in the transfer phase; however, there was a stronger decrease for the HB motion group. T_L was similar for both groups at the end of the transfer phase in both roll and pitch. An asymptotic level had not yet been reached for T_L in the roll axis at the end of the transfer phase. Generally, more visual lead is generated in the pitch axis compared to the roll axis. Note that, similarly to K_v, the error bars are again much larger in the pitch axis.

A distinct difference can be observed between the motion gain values from motion groups HO and HB during the training phase. For both the roll and pitch axes, Figures 9e and 9f, respectively, motion group HO had higher motion gains compared to motion group HB, suggesting there was a big difference in how both groups utilized the motion cues. The motion gains for HB in training were very small (especially in roll), indicating pilots hardly used the motion cues. The motion gains for HO increased over the course of training in both axes. At the start of the transfer phase, motion group HO had motion gains more similar to the end of the training phase. The motion gains continued to increase during the transfer phase in both axes and for both groups. The roll motion gain for HB in the transfer phase

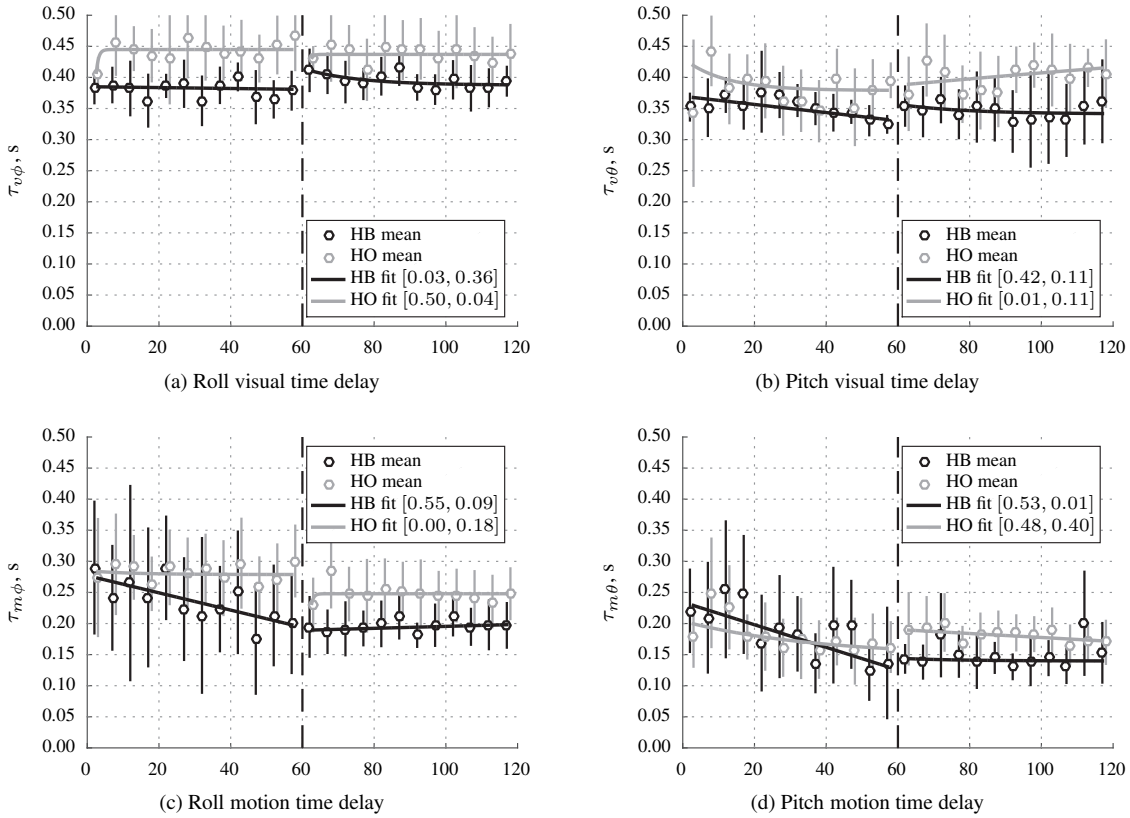

(a) Roll visual time delay

(b) Pitch visual time delay

(c) Roll motion time delay

(d) Pitch motion time delay

Figure 10. Time delays.

remained lower than the roll motion gain for HO. Motion gains were slightly higher and error bars were much larger in the pitch axis compared to the roll axis.

The delays of the pilot model are depicted in Fig. 10. Figures 10a and 10b depict the visual time delay for the controlled roll and pitch axes, respectively. For both groups, the visual time delay remained approximately constant in both axes for both the training and transfer phases. Motion group HO had higher values of τ_v for both experiment phases.

The motion time delays are depicted in Figures 10c and 10d for the roll and pitch axes. Motion group HB gradually reduced their motion time delay during training, while the motion time delays for HO remained fairly constant. The motion time delays for both groups in both axes remained constant in the transfer phase. τ_m is slightly higher for motion group HO in both axes in the transfer phase. The motion time delay is slightly lower in pitch compared to roll. Finally, the motion time delays are about 100 to 200 ms lower compared to the visual time delays.

The neuromuscular parameters are provided in Fig. 11. Figures 11a and 11b depict the neuromuscular damping values for the roll and pitch axes. In the roll axis, the neuromuscular damping appears to be much higher for the HO motion group compared to the HB motion group. In addition, the error bars for the HO motion group are also much larger. The roll neuromuscular damping in the transfer phase is similar for both groups, but seems to slightly decrease for the HB motion group. The pitch neuromuscular damping remains approximately constant for both groups in both phases of the experiment.

Figures 11c and 11d depict the neuromuscular frequencies for the roll and pitch axes. A similar difference between the groups can be observed for the neuromuscular frequencies as for the neuromuscular dampings. In the roll axis, the neuromuscular frequency is much higher for the HO motion group compared to the HB motion group. Also the error bars are much larger for HO. The roll neuromuscular frequency remained approximately constant for the training and transfer phases of the experiment. The neuromuscular frequency in roll was lower in the transfer phase compared to the training phase for HO, but slightly higher compared to the training phase for HB. The pitch neuromuscular frequency in training phase remained constant and was equal for both motion groups. Then pitch neuromuscular frequency slightly increased in the transfer phase for both motion groups, faster for HO, and more gradual for HB.

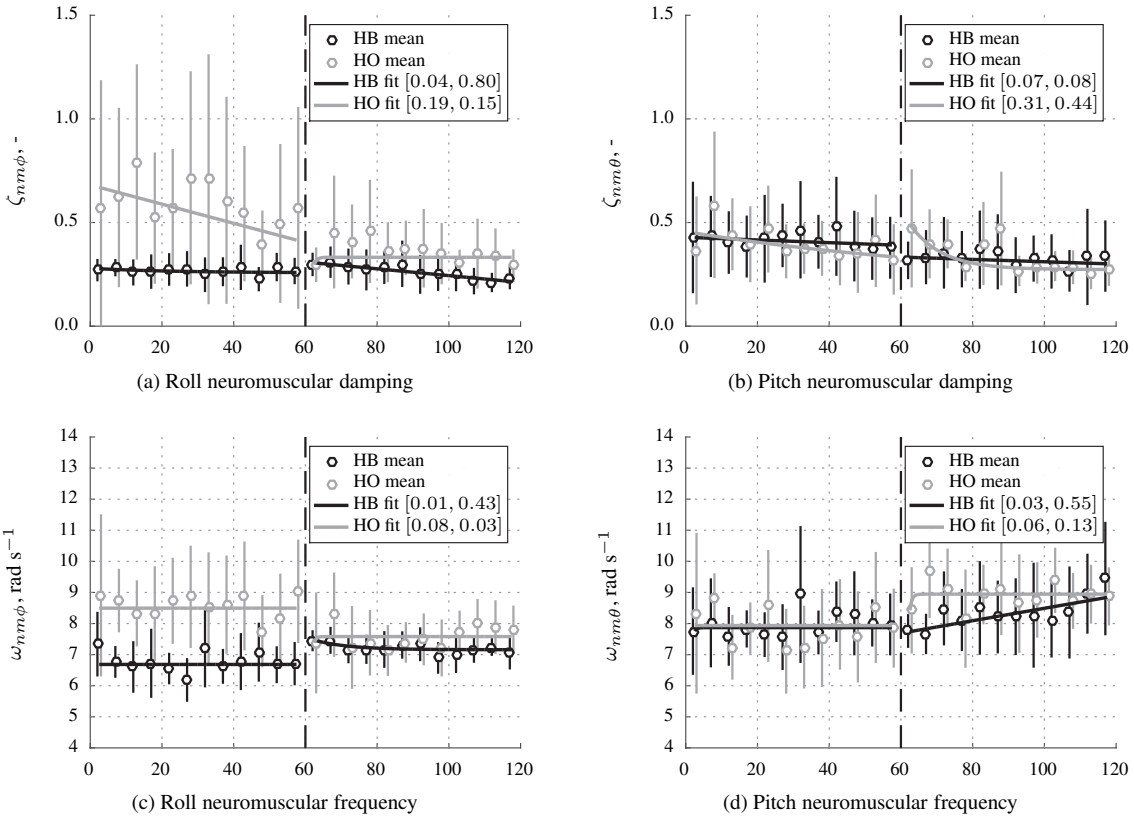

(a) Roll neuromuscular damping

(b) Pitch neuromuscular damping

(c) Roll neuromuscular frequency

(d) Pitch neuromuscular frequency

Figure 11. Neuromuscular parameters.

IV.D. Crossover Frequencies and Phase Margins

The open-loop frequency responses were calculated for both the disturbance and target forcing function inputs using Equations 5 and 6 as explained in Section II.B. The disturbance crossover frequencies and phase margins are provided in Fig. 12 for both axes. In the roll axis, the disturbance crossover frequency was significantly higher during training for motion group HO (Fig. 12a). This was accompanied by lower stability margins, as indicated by lower phase margins in Fig. 12c. After transfer, motion group HO continued with approximately the same roll disturbance crossover frequency, while motion group HB increased their crossover frequency to approximately the same level. The roll disturbance phase margins after transfer were the same as at the end of training for both groups. In the pitch axis, disturbance crossover frequencies and phase margins in the training phase were fairly constant and the same for both groups. The pitch disturbance crossover frequency was slightly higher in the transfer session for both groups and slightly increased over the course of the session (Fig. 12b). The pitch disturbance crossover frequencies for motion group HB were slightly higher than motion group HO. Pitch disturbance phase margins remained constant in the transfer phase and were slightly lower than in the training phase for both groups. Comparing roll and pitch, disturbance crossover frequencies were slightly higher and disturbance phase margins lower in roll compared to pitch for both groups in the training phase. Disturbance crossover frequencies and phase margins were similar between the two axes for both groups in the transfer phase. Note that the overall trends in the disturbance open-loop parameters are remarkably similar for both groups.

The target crossover frequencies and phase margins are given in Fig. 13 for both axes. Trends and effects are similar in both axes and for both groups. In the roll axis, the target crossover frequency decreases over the course of training and the target phase margin increases. The target crossover frequency is lower for motion group HO and, as a result, the target phase margin for this group is higher. After transfer, target crossover frequencies and phase margins were closer to the end-of-training values for motion group HB, were similar for both groups, and remained constant. Results in pitch are similar to roll for both groups in the training phase; that is, the pitch target crossover frequencies were lower for motion group HO and pitch target phase margins were higher. In contrast to the roll axis, pitch target crossover frequencies and phase margins for each group were closer to each of their respective end-of-training values.

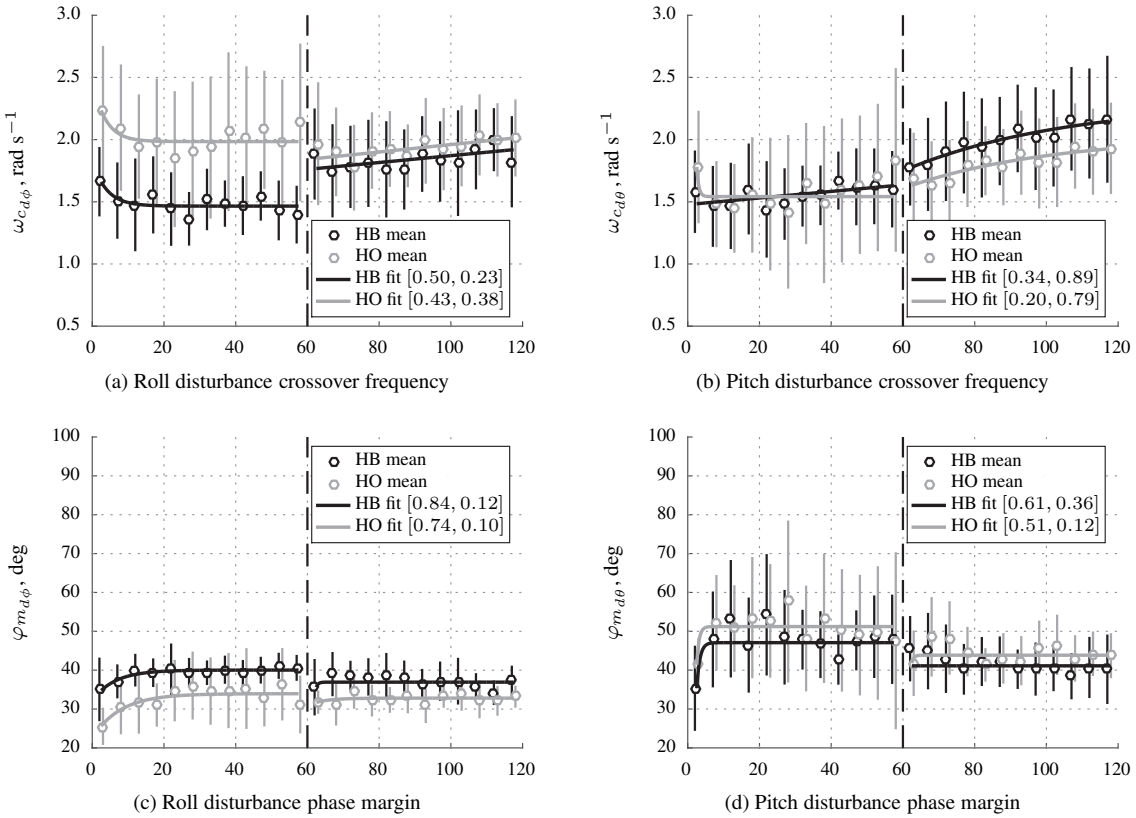

(a) Roll disturbance crossover frequency

(b) Pitch disturbance crossover frequency

(c) Roll disturbance phase margin

(d) Pitch disturbance phase margin

Figure 12. Disturbance crossover frequencies and phase margins.

For motion group HB, the pitch target phase margin slightly increased over the course of the transfer phase towards the values for motion group HO. Target crossover frequencies and phase margins were very similar between the roll and pitch axes for both groups. Only the pitch target phase margin for motion group HO throughout the transfer phase was higher in pitch compared to roll, and the pitch target crossover frequency was lower.

V. Discussion

A cybernetic approach was used to analyze the evolution of manual control behavior and performance in a multi-axis control task throughout training and after transfer of training. Previous experiments have shown that using this approach in experimental settings that are less restricted, for example, by using a multiple-axis control task instead of a single-axis control task, may result in difficulties in finding global optimum pilot model parameter estimates using MLE.[25] A transfer-of-training experiment, where the goal is to analyze participants' changing control strategy between single experimental runs, exacerbates the situation. For this reason, we still averaged five consecutive runs in the MLE procedure, a common practice in non-training experiments, increasing the chances of finding global optimum parameter sets. However, this approach might have masked some of the learning effects, especially in the beginning of the training phase, where manual control behavior adapts quickly.

Twenty-four general aviation pilots participated in the experiment. It was still difficult to find accurate parameter estimates for some, especially in the roll axis and at the beginning of the training phase. Data from five participants proved to be insufficient and were removed from the final analysis. This left nine pilots in the baseline hexapod motion group HB and ten pilots in the optimized hexapod motion group HO.

Pilots training under optimized hexapod motion HO were expected to learn faster, that is, reach asymptotic levels sooner, compared to pilots training under baseline hexapod motion HB (hypothesis H1). In addition, pilots having trained under HB were expected to need more time to adapt to the full-motion condition compared to pilots having trained under HO. Unfortunately, the different dependent measures did not unambiguously support this hypothesis, and, in fact, certain measures show faster adaptations for group HB in the training or transfer phases and others for

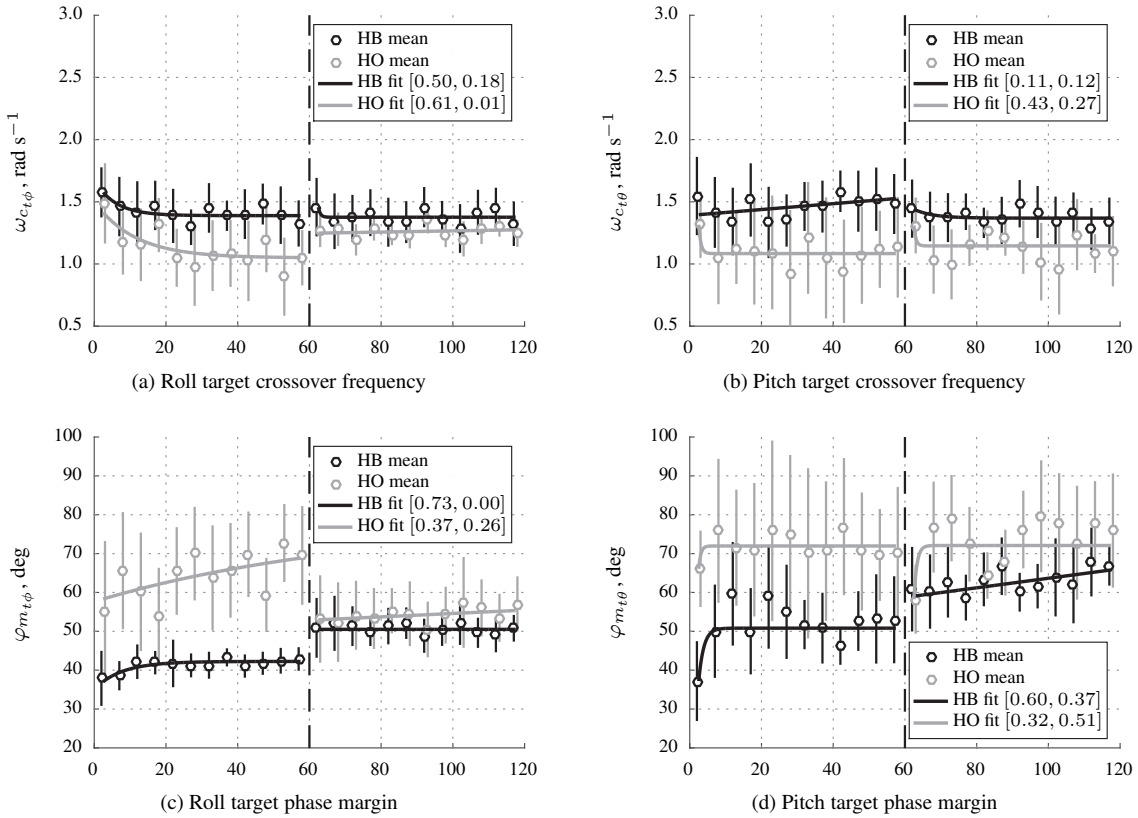

(a) Roll target crossover frequency

(b) Pitch target crossover frequency

(c) Roll target phase margin

(d) Pitch target phase margin

Figure 13. Target crossover frequencies and phase margins.

group HO. For example, the lead time constant, depicted in Fig. 9c for roll and in Fig. 9d for pitch, shows faster adaptations for group HB in the training phase, but faster adaptations for group HO in the transfer phase. The opposite is true for the motion delay, depicted in Fig. 10c for roll and in Fig. 10d for pitch. The motion time delay reaches asymptotic levels faster for group HO during the training phase, but reaches asymptotic levels slightly faster for group HB in the transfer phase.

Furthermore, at the end of transfer, several dependent measures for both groups did not converge to the same value, further invalidating hypothesis H1. For example, for the visual and motion time delays in both axes (Fig. 10), the levels at the end of transfer were different for both groups. This indicates more runs might have been required to reach asymptotic levels for some of the parameters characterizing manual control behavior, as was also found in previous quasi-transfer-of-training experiments using a cybernetic approach.[11,12] In addition, even though pilots were assigned to one of the two training-motion conditions randomly, this might point to other differences between the groups, like differences in experience. The much lower pitch control VAF for motion group HO in both the training and transfer phases, indicating this group of pilots possibly controlled less linearly, might be an indication of this. However, such differences in experience between the two groups were not readily apparent from their questionnaire data.

At the end of training, the group of pilots who trained under optimized hexapod motion HO generated less visual lead and controlled with higher gains compared to the group of pilots who trained under baseline hexapod motion HB (Fig. 9), as hypothesized in hypothesis H2. This resulted in better disturbance-rejection performance as observed by the higher disturbance crossover frequencies and lower disturbance phase margins, especially in the roll axis (Fig. 12). At the end of the transfer phase with full motion FM, we expected similar control behavior and performance as at the end of training for motion group HO, as the motion cues relevant to the task were simulated with the same fidelity in both motion conditions (hypothesis H2). However, this was not the case, as can be observed from the equalization parameters in Fig. 9, which still changed significantly for group HO in the transfer phase. This might indicate that the translational accelerations of the c.g. had a larger effect on roll and pitch control behavior and performance in the transfer phase than expected. Finally, previous research on the effects of motion cues on human operator control

behavior showed minimal variations in human limitation parameters between different motion conditions; however, in the current experiment larger variations were found (Figures 10 and 11).

VAF values were generally lower compared to previous single-axis experiments, as hypothesized in H3 (Section III.B), indicating that pilots behaved less linearly, most likely due to the periodic sampling between the roll and pitch axes. However, this did not necessarily result in smaller motion or learning effects, as variations in some parameters were substantial, for example in pilots' equalization parameters (Fig. 9). Motion and learning effects might have been less consistent for some parameters, resulting in larger error bars. Effects seemed to be slightly more pronounced in pitch compared to roll (hypothesis H4), as seen by the larger variations in pilot equalization parameters in pitch compared to roll. However, the error bars for the equalization parameters in pitch are also much larger, indicating more variability between pilots.

Some of the trends observed in the dependent measures cannot readily be explained. An example is the reduction in roll neuromuscular damping for group HB in the transfer phase (Fig. 11a). Some pilots indicated that they regularly significantly changed their control strategy over the course of the training or transfer phases, despite being told not to do so. This also resulted in irregular trends (that is, not following a learning curve) and larger error bars. One of the problems causing this might have been the score provided to pilots after each run in the lower right corner of the PFD. This score was a combination of roll and pitch RMS values. However, from the score it was not clear if a better or worse performance was a result of better or worse performance in roll or pitch, causing pilots to often feel confused about how their control strategy resulted in a certain score. This might have resulted in pilots regularly changing their control strategy and, for example, their emphasis on controlling one axis over the other.

Pilots trained for the task in 60 runs performed on a single day, and then performed the task for another 60 runs during a transfer session the following day. This training and transfer schedule was chosen to facilitate the scheduling of pilots. However, previous research has shown that this is not the most optimal way to train for skill-based tasks. A better training strategy is to spread out training over longer periods of time with longer time intervals between training sessions.[9] This might also have led to some of the inconsistencies and variability in the results.

Even though the roll and pitch controlled dynamics didn't have any cross coupling, cross coupling in manual control behavior and performance was most likely still present, as found in previous studies with similar control tasks.[18,24,25] Analyzing the extend of this cross coupling, for example, using the method described in Ref. 18, might give additional insights, and might help explain some of the results found in this study. The current study was set up to do this analysis; however, this was beyond the scope of this paper and might be attempted in the future. In addition, identification techniques for time-varying human control behavior might give more insights into control behavior adaptations over time due to training and might give more accurate parameter estimation results for single runs.[26] The development of such identification techniques is underway and will be applied to future quasi-transfer-of-training experiments.

Finally, even though the adaptations of control behavior and performance during the training and transfer phases did not unambiguously point to one motion condition providing the best training for the multi-axis task used in this experiment, insights were gained into the adaptation of pilot control behavior under different motion conditions. Furthermore, valuable lessons were learned that allow us to improve the adopted approach for future transfer-of-training studies.

VI. Conclusions

A cybernetic approach gave insights into how pilots' use of visual and motion cues in a roll-pitch control task developed for two different hexapod training-motion conditions over the course of training and after transfer to a full-motion condition in a quasi-transfer-of-training experiment. The current results do not point to one of the hexapod motion conditions for better training and transfer of training of the used multi-axis control task. However, the optimized hexapod motion condition did allow pilots to generate less visual lead, control with higher gains, and have better disturbance-rejection performance at the end of the training session compared to the baseline hexapod motion condition. Significant adaptations in control behavior still occurred in the transfer phase under the full-motion condition for both groups. Pilots behaved less linearly compared to previous single-axis control-task experiments; however, this did not result in smaller motion effects or learning effects. Motion and learning effects did seem to be more pronounced in pitch compared to roll. Finally, valuable lessons were learned that allow us to improve the adopted approach for future transfer-of-training studies.

Acknowledgments

The authors thank everyone at NASA Ames SimLabs who contributed to the experiment. We especially thank Emily Lewis and Steve Norris for their valuable contributions. This work was supported by NASA's Technologies for Airplane State Awareness project for which Dr. Gautam Shah is the technical program coordinator.

References

[1]Hosman, R. J. A. W., Hamman, B., Lehman, C., Pelchat, Y., and Schroeder, J. A., "Summary of the Panel Discussion on Motion Cueing Requirements," *Proceedings of the AIAA Modeling and Simulation Technologies Conference and Exhibit, Montreal, Quebec, Canada*, No. AIAA-2001-4253, 6–9 Aug. 2001.

[2]Schroeder, J. A. and Grant, P. R., "Pilot Behavioral Observations in Motion Flight Simulation," *Proceedings of the AIAA Guidance, Navigation, and Control Conference and Exhibit, Toronto (ON), Canada*, No. AIAA-2010-8353, 2–5 Aug. 2010.

[3]Zaal, P. M. T., Schroeder, J. A., and Chung, W. W., "Objective Motion Cueing Criteria Investigation Based on Three Flight Tasks," *The Aeronautical Journal*, Vol. 121, No. 1236, Feb. 2017, pp. 163–190.

[4]Zaal, P. M. T., Pool, D. M., de Bruin, J., Mulder, M., and van Paassen, M. M., "Use of Pitch and Heave Motion Cues in a Pitch Control Task," *Journal of Guidance, Control, and Dynamics*, Vol. 32, No. 2, March–April 2009, pp. 366–377.

[5]Pool, D. M., Zaal, P. M. T., van Paassen, M. M., and Mulder, M., "Effects of Heave Washout Settings in Aircraft Pitch Disturbance Rejection," *Journal of Guidance, Control, and Dynamics*, Vol. 33, No. 1, Jan.–Feb. 2010, pp. 29–41.

[6]Zaal, P. M. T. and Zavala, M. A., "Effects of Different Heave Motion Components on Pilot Pitch Control Behavior," *AIAA Modeling and Simulation Technologies Conference*, American Institute of Aeronautics and Astronautics (AIAA), jun 2016.

[7]McRuer, D. T. and Jex, H. R., "A Review of Quasi-Linear Pilot Models," *IEEE Transactions on Human Factors in Electronics*, Vol. HFE-8, No. 3, Sept. 1967, pp. 231–249.

[8]Stapleford, R. L., Peters, R. A., and Alex, F. R., "Experiments and a Model for Pilot Dynamics with Visual and Motion Inputs," Tech. Rep. NASA CR-1325, NASA, 1969.

[9]Levison, W. H., Lancraft, R. E., and Junker, A. M., "Effects of Simulator Delays on Performance and Learning in a Roll-Axis Tracking Task," *Fifteenth Annual Conference on Manual Control*, Wright State University, Dayton (OH), 20–22 March 1979, pp. 168–186.

[10]Zaal, P. M. T., Popovici, A., and Zavala, M. A., "Effects of False Tilt Cues on the Training of Manual Roll Control Skills," *Proceedings of the AIAA Modeling and Simulation Technologies Conference, Kissimmee, Florida FL*, No. AIAA-2015-0655, 5–9 Jan. 2015.

[11]Pool, D., Harder, G., Damveld, H., van Paassen, M., and Mulder, M., "Evaluating Simulator-Based Training of Skill-Based Control Behavior using Multimodal Operator Models," *Proceedings of the 2014 IEEE International Conference on Systems, Man, and Cybernetics, San Diego, CA*, 5–8 Oct. 2014, pp. 3132–3137.

[12]Mendes, M. S. F., Pool, D. M., and van Paassen, M. M., "Effects of Peripheral Visual Cues in Simulator-Based Training of Multimodal Control Skills," *Proceedings of the AIAA Modeling and Simulation Technologies Conference, Denver, Colorado CO*, 2017.

[13]McRuer, D. T., Graham, D., Krendel, E. S., and Reisener, W., "Human Pilot Dynamics in Compensatory Systems. Theory, Models and Experiments With Controlled Element and Forcing Function Variations," Tech. Rep. AFFDL-TR-65-15, Wright Patterson AFB (OH): Air Force Flight Dynamics Laboratory, 1965.

[14]Jex, H. R. and Magdaleno, R. E., "Roll Tracking Effects of G-vector Tilt and Various Types of Motion Washout," *Fourteenth Annual Conference on Manual Control*, University of Southern California, Los Angeles (CA), 25–27 April 1978, pp. 463–502.

[15]Beard, S. D., Reardon, S. E., Tobias, E. L., and Aponso, B. L., "Simulation System Optimization for Rotorcraft Research on the Vertical Motion Simulator," *Proceedings of the AIAA Modeling and Simulation Technologies Conference, Minneapolis (MN)*, 13–16 Aug. 2012, Paper no. AIAA-2012-4634.

[16]Dieudonne, J. E., Parrish, R. V., and Bardush, R. E., "An Actuator Extension Transformation for a Motion Simulator and an Inverse Transformation Applying Newton-Raphson's Method," NASA Technical Note NASA TN D-7067, NASA Langley Research Center, Nov. 1972.

[17]International Civil Aviation Organization, *ICAO 9625: Manual of Criteria for the Qualification of Flight Simulation Training Devices. Volume 1 – Aeroplanes*, 2009, 3rd edition.

[18]Barendswaard, S., Pool, D., and Mulder, M., "Human Crossfeed in Dual-Axis Manual Control with Motion Feedback," Tech. rep., Delft University of Technology, 2016.

[19]Damveld, H. J., Beerens, G. C., van Paassen, M. M., and Mulder, M., "Design of Forcing Functions for the Identification of Human Control Behavior," *Journal of Guidance, Control, and Dynamics*, Vol. 33, No. 4, July – Aug. 2010, pp. 1064–1081.

[20]Danek, G. L., "Vertical Motion Simulator Familiarization Guide," NASA Technical Memorandum NASA TM-103923, NASA, 1993.

[21]Zaal, P. M. T., Pool, D. M., Chu, Q. P., van Paassen, M. M., Mulder, M., and Mulder, J. A., "Modeling Human Multimodal Perception and Control Using Genetic Maximum Likelihood Estimation," *Journal of Guidance, Control, and Dynamics*, Vol. 32, No. 4, July–Aug. 2009, pp. 1089–1099.

[22]Shirley, R. S. and Young, L. R., "Motion Cues in Man-Vehicle Control," *IEEE Transactions on Man Machine Systems*, Vol. 9, No. 4, Dec. 1968, pp. 121–128.

[23]Pool, D. M., Zaal, P. M. T., Damveld, H. J., and van Paassen, M. M. M. M., "Evaluating Simulator Motion Fidelity using In-Flight and Simulator Measurements of Roll Tracking Behavior," *Proceedings of the AIAA Modeling and Simulation Technologies Conference, Minneapolis (MN)*, No. AIAA-2012-4635, 13–16 Aug. 2012.

[24]Zaal, P. M. T., "Manual Control Adaptation to Changing Vehicle Dynamics in Roll-Pitch Control Tasks," *Journal of Guidance, Control, and Dynamics*, Vol. 39, No. 5, May 2016, pp. 1046–1058.

[25]Zaal, P. M. T. and Pool, D. M., "Multimodal Pilot Behavior in Multi-Axis Tracking Tasks with Time-Varying Motion Cueing Gains," *Proceedings of the AIAA Modeling and Simulation Technologies Conference, National Harbor (MD)*, No. AIAA-2014-0810, 13–17 Jan. 2014.

[26]Popovici, A., Zaal, P. M. T., and Pool, D. M., "Dual Extended Kalman Filter for the Identification of Time-Varying Human Manual Control Behavior," *Proceedings of the AIAA Modeling and Simulation Technologies Conference, Denver, Colorado CO*, 2017.